Comprehensive Measurement-Based Evaluation of Posture Detection from Ultra Low Power UWB Signals

Robert Heyn and Armin Wittneben
Wireless Communications Group, ETH Zurich, Switzerland
{heyn, wittneben}@nari.ee.ethz.ch

***Abstract*—Due to the ever-increasing life expectancy, extending the autonomy of elderly people is of great social importance. Posture detection can be a crucial element here. An example of particular significance is fall prevention, whereby critical postures are detected before a fall occurs – in any environment.**

An on-body posture detection system based on wireless signaling is particularly attractive because it is lightweight, not obstructive, and promotes a ubiquitous use as it does not require any off-body infrastructure. Due to the manifold of human physiques and living environments (i.e. signal propagation and multipath conditions), posture detection based on wireless signals is very challenging. The feasibility of such a system for an extensive set of postures has not been demonstrated and appropriate comprehensive wideband on-body matrix channel measurements are missing. This paper tries to fill this void. We first define an extensive set of postures related to fall prevention. For these 43 postures we perform a large-scale measurement campaign of (18x18) channel impulse response (CIR) matrices between 18 on-body nodes. In order to make the results as representative as possible, we intentionally include variation in each posture and consider various test subjects and indoor environments. The posture detection performance is evaluated for two metrics: (i) total energy of the CIR (ultra low complexity), and (ii) magnitude of CIR (very low complexity). We investigate suitable choices of carrier frequency and bandwidth, and demonstrate that ultra low transmit power wireless posture detection is feasible under real-world constraints for an extensive set of postures.

***Index Terms*—posture detection, UWB, WBAN, fall prevention**

I. Introduction

Technical and medical advancements in recent years have enabled personalized and technology-supported healthcare. For the growing number of elderly citizens, an application of interest is fall prevention, which provides increased safety from a common source of injuries [1] while living independently. In contrast to fall *detection*, i.e. identifying when a fall has happened, fall *prevention* systems aim at detecting fall-prone situations in order to initiate protective measures, like e.g. an acoustical stimulus, in order to prevent the fall.

In addition to camera-based systems [2] and accelerometers [3], radio waves have been identified as a means to monitor a patient's posture in order to detect fall risks [4]. Baird et al. [5] detect human postures based on UWB radar signals with acceptable confidence for a very limited set of postures without major variations. Like for camera-based systems, the scope of operation is limited to locations with appropriate external infrastructure. Wearable systems overcome this limitation.

Advantages of wireless systems include the additional use for sensor data transmission, the possibility for radar-based obstacle detection, and their privacy-preserving nature in contrast to camera-based solutions. A wearable system based on a wireless body area network (WBAN) allows for constant monitoring in any environment, as it does not rely on fixed infrastructure. However, battery-powered nodes pose a constraint to its power consumption. Furthermore, the variable wireless channels around a human body in various environments are challenging for radio-based systems.

These wireless channels between on-body WBAN nodes have been subject to extensive research. Zhang and Li [6] conduct measurements with a focus on communication channel parameters and suitable pulse shapes. Wang et al. [7] simulate a channel model for a variety of generic postures and verify it with measurements in an anechoic chamber. An office room as a more realistic environment for measurements was chosen by Lu et al. [8], who further consider test subjects of different physique for a statistical channel analysis.

Communication-focused applications benefit from stable channel conditions with low path loss. In order to utilize WBAN signals for posture detection, it is crucial that the on-body channels differ between the postures, as variations in certain characteristics make the channels distinct depending on the body posture. Several approaches towards posture detection with WBANs have been presented. Quwaider et al. [9] propose a system based on narrowband RSSI measurements from low-cost on-body nodes operating at $433\,\mathrm{MHz}$ combined with accelerometers, to coarsely classify postures into four activities (sit/stand/walk/run). Paschalidis et al. [10] detect body postures based on the RSSI at $2.4\,\mathrm{GHz}$. Their approach, however, requires a vast amount of training data to obtain probability density estimates for a generalized likelihood test. Yang et al. [11] use Random Forests for posture detection from measurements of the frequency response of WBAN channels at $2.45\,\mathrm{GHz}$. In an office environment, they achieve an accuracy of $74\,\%$ for their limited set of 18 postures.

In our previous work [12], we have introduced a WBAN concept for posture detection with low complexity least-squares approaches and evaluated its feasibility with measurements. However, the measurements were conducted under

TABLE I: Overview of ADL Postures

group	postures	description	example situation
stand	2	upright, arms down/bent	kitchen work
	2	arm extended forward	taking item from shelf
	3	arm(s) up	getting dressed, phone call
	3	bending, arm(s) down	picking item from ground
walk	6	step snapshots	walking on even ground
	4	step snapshots on stairs	walking on stairs
sit	1	leaning back, arms in lap	relaxing
	3	upright, arms bent/raised	reading, eating
	3	sitting down/standing up	transition sit-stand
	1	leaning forward, arms down	wearing shoes

TABLE II: Overview of Fall Postures

group	postures	description
fall forward	4	arms stretched forward
	1	arms downwards
	1	arms raised
	1	arms backwards
fall backward	1	arms forward
	1	arms back
	4	arms down/sideways
fall sideways	2	towards right/left

idealized conditions in an anechoic chamber without variation within the postures. Furthermore, the data only comprised a small selection of nine postures, which were performed by a single test person. Consequently, the findings can only be generalized to a limited extent.

In this work, we aim to verify the previous findings and generalize them in order to take the next step towards WBAN-based posture detection for fall prevention. We describe a large-scale measurement campaign in a more realistic indoor environment with multiple test subjects and changing surroundings. The acquired data provides a solid foundation for the evaluation of posture detection algorithms in generic indoor environments. The UWB measurements further allow an analysis of a suitable frequency range and thus a basis for the selection of favorable physical layer implementations.

The remainder of this paper is structured as follows: Section II introduces the selection of postures for the fall prevention context. Section III provides a description of the measurement process. Section IV outlines some characteristics of the acquired data. Posture detection processing is introduced in Section V, results are discussed in Section VI. Section VII concludes the paper.

II. Posture Selection

The most important functionality of fall prevention systems is to distinguish fall-prone situations from activities of daily living (ADL). In addition to this distinction, an identification at a finer granularity level is useful: For instance, the update rate of the system can be decreased while sitting, as falls are more likely to happen when the patient is standing or walking [13]. A precise recognition of a particular posture provides information about the weight distribution and the arm position of the patient, which is useful for initiating countermeasures against an imminent fall. In the following, we distinguish *categories* (ADL/fall-related), *groups* (stand/walk/sit, falling forward/backward/sideways) and each separate *posture*.

A. Postures of Activities of Daily Living (ADL)

The first category we will describe in detail comprises postures of common activities of daily living (ADL) of elderly residents. The postures and their variations are selected such that at least one posture of each of the most common daily tasks (which typically comprise several postures) is covered. Note that sports activities are not included in our selection. Tab. I summarizes the ADL postures.

1) Standing Postures: The group of standing postures in our selection comprises ten different postures. For both the upright standing postures additional measurements are taken with a chair behind and a table in front, with a metal chair in front (simulating a walking aid) and in front of a table counter.

2) Walking Postures: The second group of ADL postures includes ten walking snapshots. We split a single step into three posture snapshots, resulting in six postures for a full walking cycle. Identifying the phase of a step, i.e. the particular leg position, can be important for fall prevention as it allows to infer the patient's weight distribution, which can help to anticipate the fall direction and/or adapt the respective countermeasures such as a muscle stimulus. In addition to walking on even ground, we consider postures for climbing up and down stairs, each with either foot forward, resulting in four additional postures.

3) Sitting Postures: Although the risk of an immediate fall is reduced while sitting, it is important to include sitting postures in the calibration data in order to avoid false positives. We distinguish 8 sitting postures, including 3 postures occurring during the process of standing up/sitting down: Forwards from a free-standing chair and forwards/sideways with support from a table. Additional measurements for the upright sitting postures are taken with a table in front of the person.

B. Fall-Related Postures

We group the fall-related postures by the direction of the imminent fall as shown in Tab. II. Knowing the fall direction enables suitable countermeasures, such as triggering a selective muscle stimulus to prevent the fall or launching an appropriately placed wearable airbag.

1) Falling Forward: Tripping over small objects or steps is likely to result in a forward fall. Our selection of forward-falling postures mainly differ in the orientation of the arms. Leaning towards one side, e.g. during a turn, may result in a fall towards a forward-left or forward-right direction, which is also covered in our posture selection.

2) Falling Backward: An incorrect shift of body weight is another common cause for falls [13], which can also happen in a backward direction. Our selection contains six backward falling postures with different arm positions, while the knees are slightly bent for all of the postures.

3) Falling Sideways: Lastly, we include two postures related to sideways falls. As falls towards forward-left, forward-right as well as backward-left and backward-right have been

included previously, only the direct fall towards either side is considered here.

C. Posture Variations

It is intuitive that sitting postures differ significantly from walking or falling postures. However, more similar postures pose a challenge to posture detection systems: On one hand, robustness of the detection towards small variations within every posture is desired to avoid overfitting to particular posture realizations. On the other hand, there are similar postures which need to be distinguished in the classification.

As an illustrative example for desired posture variation within a single posture, consider an upright standing posture with one arm raised towards the head. We consider different activities to be variations of this posture, e.g. eating (hand in front of the head), making a phone call (hand at the ear), or styling hair (hand on top of the head). When a distinction between these variations is important for the application, they must be regarded as separate postures. In other scenarios such as fall prevention, a distinction between the variations is not required and thus causes unnecessary calibration overhead. Consequently, all these variations are considered as the same posture in our case. The procedure to capture such variations in the measurements is described in Section III-D.

As an example of a relevant small variation between two postures, consider a walking snapshot where legs are parallel: One leg bears the weight, the other is parallel and moves forward in order to make the next step. This posture is very similar for both a step with the left and with the right leg. However, it is required to distinguish between these two variants, as the weight distribution of the user is entirely different, i.e. all the weight is on the left or right leg, respectively. The phase of gait needs to be taken into account for fall prevention, and detecting the separate postures is helpful for time series analysis. Consequently, we consider these variations as separate postures.

III. Measurements

Ideally, data collection would comprise measurements during a wide variety of activities and falls over multiple days in diverse environments for multiple users to obtain a truly representative dataset. As this is infeasible with our measurement system (cf. Section III-A), we aim to cover extreme cases w.r.t. environment (open space vs. densely cluttered, Section III-B) and test subjects (male/female and height/weight difference, Section III-C) in order to make our dataset and the findings of this work as representative as possible.

A. Hardware

The measurement equipment for data acquisition is identical to our previous measurements in an anechoic chamber [12]. Frequency domain data is recorded using a R&S ZNBT8 Vector Network Analyzer (VNA) [14] and 18 body-mounted planar UWB dipoles on torso and limbs, whose placement is illustrated in Fig. 1. Concurrent measurements allow reproducible postures and data acquisition within a reasonable time.

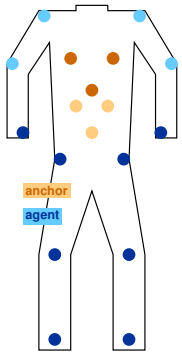

Fig. 1: Antenna placement on front (dark) and back (light)

Processing is done offline after conversion to the time domain using an IFFT. Tab. III summarizes the VNA configuration.

It must be pointed out that the linearly polarized dipoles are suboptimal for our application: A minor change in the posture can induce a rotation of the polarization axis of an antenna. As a consequence, the amplitude of links to a particular node can vary significantly, which causes strongly deviating measurement results for minor variations of the same posture. An intuitive soultion for this shortcoming is the usage of circularly polarized antennas. However, in this work we use a different approach by constantly varying every posture within reasonable boundaries across several measurements (cf. Section III-D). This way we consider multiple relevant relative antenna orientations for every posture.

B. Environment

Fall prevention systems must operate reliably in a variety of environments ranging from outdoor areas to public transport and indoor surroundings. Differences in the wireless channels of these environments, especially multipath propagation, influence the measured on-body channels. An exhaustive analysis of all possible environments is not feasible. Consequently, we focus on indoor measurements in this work, as our target user group of old people spends the majority of time indoors. The environment for measurements is a furnished office, whose floor plan with the measurement area is shown in Fig. 2.

In order to account for changing indoor surroundings, we introduce variety in the measurements modifying the immediate surroundings within the same office room. In an *open environment*, the test subject performs all postures in the center of an empty space with a distance of at least $1.5\,\mathrm{m}$ to all reflecting items. In a *cluttered environment*, various

TABLE III: VNA Configuration

parameter	**symbol**	**value**
minimum frequency	f_{min}	$2.5\,\mathrm{GHz}$
maximum frequency	f_{max}	$8.5\,\mathrm{GHz}$
resulting sweep bandwidth	B	$6\,\mathrm{GHz}$
number of frequency sweep points	N_{f}	1501
resulting frequency step	Δf	$4\,\mathrm{MHz}$
resolution bandwidth	RBW	$1\,\mathrm{MHz}$
output power	P_{out}	$0\,\mathrm{dBm}$

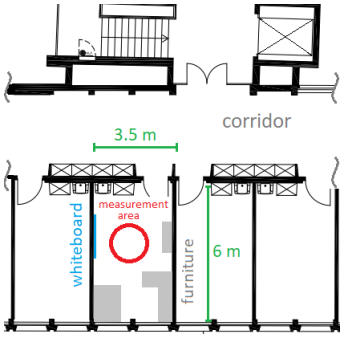

Fig. 2: Floor plan of the office environment with fixed furniture. Additional items were placed close to the test person in the measurement area (red) for the *cluttered environment*.

TABLE IV: Test Subject Data

test person	P1	P2	P3
sex	female	male	male
age	24 yrs.	29 yrs.	25 yrs.
height	1.58 m	1.78 m	1.90 m
weight	55 kg	70 kg	94 kg

reflecting/scattering items are placed in immediate vicinity of the test person, i.e. within 1 m radius. Metallic sheets, tripods, a standing fan with a protecting metallic cage, and the VNA placed on a rolling cart serve as reflectors/scatterers in various constellations and are subsequently jointly referred to as "clutter". Clutter constellations differ for the test subjects.

C. Test Subjects

All posture measurements are conducted for three test persons (P1-P3, see Tab. IV). Despite the similar age of the test subjects, the characteristics of their physique differ. In particular, the distances between TX and RX antennas depend on the height and limb length, whereas the overall shape of the body influences the shadowing conditions and the wave propagation around the torso [8]. The variety in the human body characteristics covered with the three subjects enables both a comparison (for subject-dependent results) as well as a generalization (for subject-independent results) of the findings. In the remainder of this work, we use data from all test subjects unless stated otherwise.

D. Posture Variation Measurement

The channel matrix for every posture is measured 12 times (i.e. 12 snapshots) for each environment and test person, covering small and larger scale variations of the respective posture. Throughout the process of performing a posture, the test person moves their limbs within a range of a few centimeters (small scale variation). After every third snapshot the test person returns to a relaxed posture and takes a short break before returning to the measurement posture. Naturally the posture will differ after the pause, which introduces the desired large scale variation. This "reset" to a relaxed posture (in addition to conscious variations of the posture where possible) ensures a more representative variation in the snapshots.

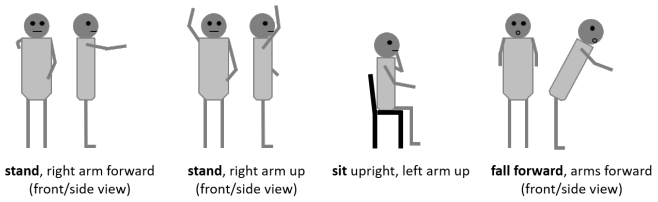

(a) Selected postures

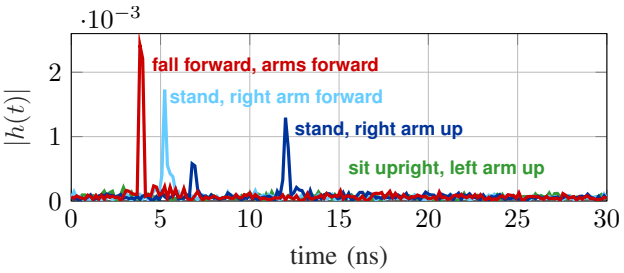

(b) Magnitude of CIR

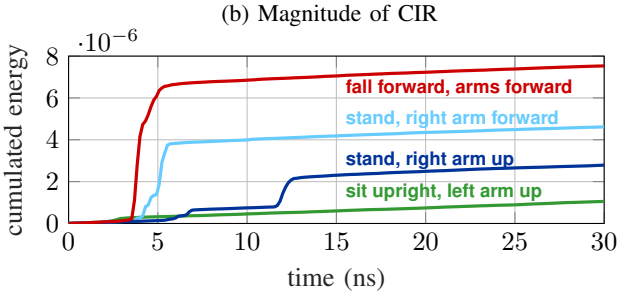

(c) Cumulated energy

Fig. 3: LOS/NLOS for right wrist-ankle link

IV. Observations

Ideally, the measured CIRs have little variation within measurements of a single posture in different environments, and significant differences between different postures to make them distinct from one another. In the following, we will present some observations in the collected data related to the signal propagation and discuss their influence for the posture detection task at hand.

A. Line of Sight (LOS)

In order to illustrate the strong impact of the LOS conditions on the CIRs, we take a closer look at the link between the right wrist and the right ankle for 4 different postures, which are shown in Fig. 3a. Fig. 3b shows the magnitude of the respective CIR over the first 30 ns for test person P3 in the open environment. The cumulated energy $E(t) = \int_0^t |h(\tau)|^2 d\tau$ is shown in Fig. 3c.

We observe that the characteristics of this link vary significantly between the postures: A strong LOS path without additional multipath components (MPCs) characterizes the channel for the postures with the arm extended forward. The LOS path also occurs for the standing posture with raised arm. The additional MPC for this posture is the reflection from the metallic whiteboard mounted on the office wall. Apparently

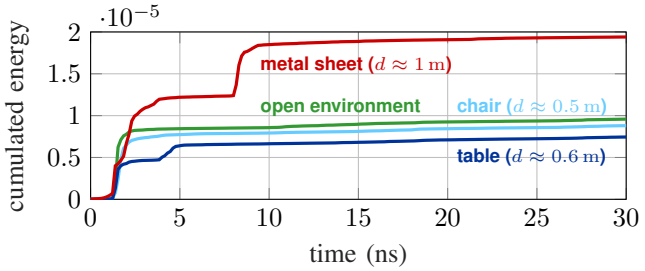

Fig. 4: Cumulated energy of knee-ankle link with different objects in front of the test person

the specific orientation of TX and RX antenna in this posture favors this path such that it exhibits a higher amplitude than the LOS path. In case of the sitting posture, the low link energy in spite of the short delay indicates a NLOS situation. It is intuitive that the more a link varies between postures, the higher is its contribution to the distinction of these postures.

B. Multipath from Objects in the Environment

As an illustrative example for the influence of the environment, we take a look at an affected link for one of the upright standing postures. Our data includes multiple measurements of the same posture (standing, arms bent) performed by test person P1 with and without various metallic items in front of the leg. The cumulated energy for the link between the left knee and the left ankle is shown in Fig. 4.

The metal-frame chair (light blue line in Fig. 4) does not cause a visible second MPC, and the CIR is very similar to the one in the open environment (green). A table with a single thick metallic leg (dark blue) provides a weak second path with a delay of approximately $4\,\mathrm{ns}$ in addition to the LOS. A vertical metal sheet leaning to a wall (red) acts as a strong reflector, which induces a stronger second MPC with a path delay of approximately $8\,\mathrm{ns}$. This result is well in line with the expectations of weaker reflections from the round legs of furniture and a strong echo from the metal sheet. Such an influence of the environment on measurements of the same posture demonstrates the need to take different surroundings into account, where our diverse choice of clutter covers a variety of real-world items and emphasizes extremes (especially the strongly reflecting metal sheet), thus serving as a worst case consideration.

V. Processing

Our envisioned fall prevention system consists of (i) a wireless measurement sub-system, which generates a temporal sequence of estimates of the instantaneous posture, and (ii) an application-specific posture monitoring subsystem, which incorporates one or multiple estimates and may include additional side information such as data from an Inertial Measurement Unit (IMU). This paper considers only the wireless subsystem, which consists of 18 on-body nodes, namely 12 agents on the limbs and 6 anchors on the torso (cf. Fig. 1). The agents transmit individual pseudorandom noise (PN) sequences with a bandwidth B and the maximum TX power spectral density permitted by the UWB regulations ($-41.3\,\frac{\mathrm{dBm}}{\mathrm{MHz}}$). Receivers at the anchor nodes estimate the CIR of the agent-anchor link via a correlation with the respective PN sequences. For posture detection we use two noncoherent nearest-neighbor-approaches with normalized least-squares-metrics as introduced in [12]: Anchors either measure the magnitude of the CIR ($|h(t)|$, "*MagCIR*") or only its energy ($\int |h(t)|^2 dt$, "*RSS*"). The latter approach can also be implemented with UWB Impulse Radio and an energy detector receiver. The anchors forward the channel measurements to a central unit for posture recognition.

The training set requires at least one measurement for every posture to be detected during deployment. In an offline training phase, the user performs each posture once, and the respective measurements are saved and used for comparison with the incoming test measurements during online operation. In this work, we only use a single measurement per posture for each environment (open/cluttered) for training and the remaining 11 measurements per posture and environment for testing.

Battery-powered WBANs require low power consumption for long-term ubiquituous operation. Consequently, reducing the transmit power of nodes is an important goal. Extensive measurements with different power levels are not required to analyze the influence of variations of the agent transmit power. Instead, we model the SNR differences by scaling the noise level: For every test CIR, we determine the average noise power during an interval without measurable signal contributions ($t > 40\,\mathrm{ns}$). Additive white Gaussian noise (AWGN) with the appropriate variance is added to scale the SNR in the same way as a reduction of the VNA output power.

In order to put the system proposal and the (noisy) VNA measurements with the configuration in Tab. III in perspective, we demand equal energy E for a representative CIR measurement over the bandwidth $\tilde{B}$ with the VNA and using a PN sequence:

$$E_{\mathrm{VNA}} = \underbrace{\frac{\tilde{B}}{\Delta f}}_{=\tilde{N}_{\mathrm{f}}} \underbrace{\frac{1}{\mathrm{RBW}}}_{=T_{\mathrm{meas}}} P_{\mathrm{out}} \stackrel{!}{=} T_{\mathrm{PN}}\, P_{\mathrm{PN}} = E_{\mathrm{PN}}, \qquad (1)$$

where T_{meas} denotes the duration of the VNA measurement per frequency bin, and T_{PN} and P_{PN} are the duration and the agent transmit power for the PN sequence, respectively. With the resulting power spectral density for the PN sequence

$$\mathrm{PSD}_{\mathrm{PN}} = \frac{P_{\mathrm{out}}}{\mathrm{RBW} \cdot \Delta f \cdot T_{\mathrm{PN}}} = \frac{P_{\mathrm{PN}}}{\tilde{B}} \stackrel{!}{=} -41.3\,\frac{\mathrm{dBm}}{\mathrm{MHz}}, \qquad (2)$$

we obtain a PN sequence duration of $T_{\mathrm{PN}} \approx 3.4\,\mathrm{ms}$ for $P_{\mathrm{out}} = 0\,\mathrm{dBm}$ and $\tilde{B} = 1\,\mathrm{GHz}$, which corresponds to an average agent TX power of $\bar{P}_{\mathrm{TX}} = 2.5\,\mu\mathrm{W}$ assuming 10 measurements per second, which we consider sufficient for continuous posture monitoring. Scaling the VNA output power to e.g. $P_{\mathrm{out}} = -10\,\mathrm{dBm}$ corresponds to a shorter PN sequence and thus an average TX power of $\bar{P}_{\mathrm{TX}} = 0.25\,\mu\mathrm{W}$. Consequently, the VNA measurements provide a solid basis for the evaluation of a system with battery-powered agents.

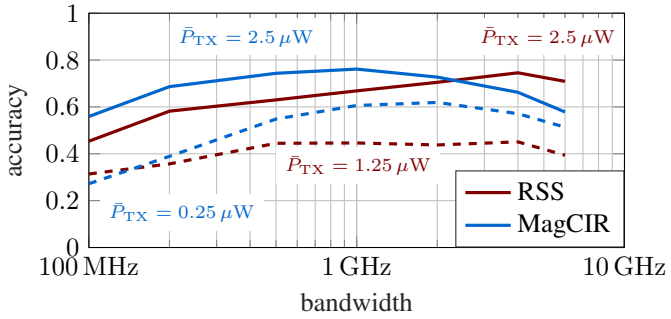

Fig. 5: Accuracy vs. bandwidth for different average transmit power levels $\bar{P}_{\mathrm{TX}}$ (w.r.t. $B = 1\,\mathrm{GHz}$)

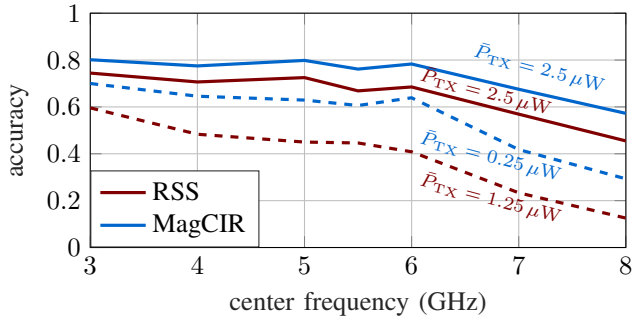

Fig. 6: Accuracy vs. center frequency for different average transmit power levels $\bar{P}_{\mathrm{TX}}$ (w.r.t. $B = 1\,\mathrm{GHz}$)

VI. Results

For an assessment of the posture detection performance, we choose the accuracy as a figure of merit, i.e. the fraction of all test cases in which the posture was detected correctly. As training and testing are done with different datasets but the same selection of postures, the theoretical accuracy limit is $100\,\%$. The accuracy for a random guess is $\approx 2\,\%$. All results consider 100 evaluation runs with individual random number generator seeds, which are used for the random training data selection and random noise realizations. Training data is not used for testing within the same evaluation.

A. Bandwidth

The system bandwidth is a crucial design parameter for wireless systems. In order to achieve a low hardware complexity, a small bandwidth is helpful. A larger bandwidth makes the CIRs more distinct by allowing a separation of multipath components, and increases the robustness against narrowband interference through frequency diversity.

For this evaluation, the center frequency is fixed to $5.5\,\mathrm{GHz}$. Two different power levels are considered for each approach: $2.5\,\mu\mathrm{W}$ (i.e. without additional noise) as well as $1.25\,\mu\mathrm{W}$ (*RSS*) and $0.25\,\mu\mathrm{W}$ (*MagCIR*), respectively. The results are displayed in Fig. 5. In case of higher transmit power, we observe that for a signal bandwidth exceeding $300\,\mathrm{MHz}$ the accuracy is in the range of $60 - 75\,\%$ for *RSS* and $70 - 80\,\%$ for *MagCIR*. Narrowband configurations perform significantly worse for both approaches. We further observe that the performance degrades with reduced transmit power: The accuracy of the *RSS* approach is around $50\,\%$ when the transmit power is halved. A shorter integration window with a demand for finer synchronization would balance this problem. The *MagCIR* approach suffers from reduced transmit power to a lower extent, which is in line with the observations in [12]. Additional bandwidth partially compensates the reduced power, with a peak accuracy of $\approx 60\,\%$ for $1 - 2\,\mathrm{GHz}$ bandwidth. We use a signal bandwidth of $1\,\mathrm{GHz}$ for all following evaluations. The accuracy further varies between the test persons (Fig. 5 shows averaged results for P1-P3): For the same parameters, the accuracy for test person P3 is about 10% lower than for P1 and P2, which is likely due to stronger posture variations during the measurement.

B. Center Frequency

In the system design process, a smart choice of the center frequency helps to avoid crowded frequency bands like the $5\,\mathrm{GHz}$-ISM band without compromising on detection accuracy. For this analysis, the signal bandwidth is fixed to $1\,\mathrm{GHz}$ while the center frequency is varied in the range of $3 - 8\,\mathrm{GHz}$. Fig. 6 shows the accuracy for both evaluation methods.

Both approaches perform better for low center frequencies, where the accuracy lies above $70\,\%$ (*RSS*) and $80\,\%$ (*MagCIR*). We again observe the trade-off between transmit power and complexity: The accuracy of the low complexity *RSS* approach with $\bar{P}_{\mathrm{TX}} = 2.5\,\mu\mathrm{W}$ is close to that of the more complex *MagCIR* approach with $\bar{P}_{\mathrm{TX}} = 0.25\,\mu\mathrm{W}$. In the following, we use a center frequency of $4\,\mathrm{GHz}$ to stay within the UWB frequency range ($> 3.1\,\mathrm{GHz}$) and to avoid interference from the crowded frequency range around $5 - 5.9\,\mathrm{GHz}$.

C. Sensitivity Towards the Environment

In order to analyze the influence of the environment on the posture detection performance, we partition the measurements into a subset taken in an open environment (cf. Section III-B) and a subset taken in a cluttered environment. We distinguish between 3 types of training data sets: (i) open only, (ii) cluttered only, and (iii) mixed. In turn, we use 2 types of test data: (i) open and (ii) cluttered. In case of matching environments for training and test, we exclude the training measurements from testing so that there is no overlap. The respective accuracy for the 6 combinations of training and test data type is shown in Fig. 7 for *RSS* and *MagCIR*.

In case of matching training and test data type (green bars) the achieved accuracy exceeds $80\,\%$. In case of mismatch, i.e. "open/clutter" or "clutter/open", the performance breaks down (red bars) with the accuracy dropping to $40\,\%$. This highlights the significant difference between the open and cluttered environments – as has been the intention. It is impressive that the mismatch loss is recovered by using the "mixed" training set type (blue bars). As a practical conclusion, calibration measurements to generate training data should be performed

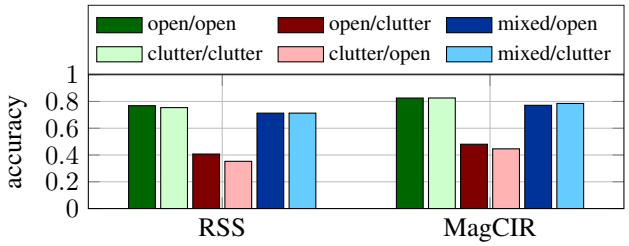

Fig. 7: Accuracy for different training/test data combinations

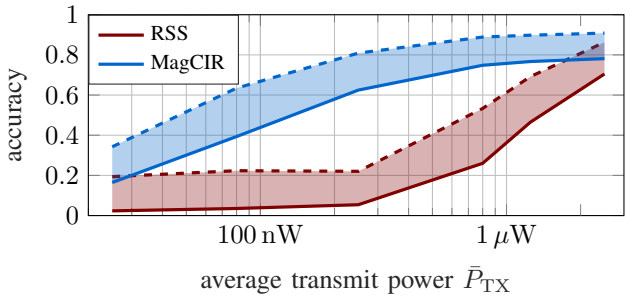

Fig. 8: Accuracy vs. transmit power (solid lines for posture detection, dashed lines for group detection)

in diverse environments in order to obtain robustness towards changes of the surroundings.

D. Severity of Errors

Not all applications require an distinction of all the (partially very similar) postures, e.g. there may be situations in which a detection of the activity (stand/walk/sit) or the direction of the fall (forward/backward/sideways) is sufficient. We can account for such cases by adapting the weight given to detection errors within the groups (intra-group error weights), ranging from 0 (classification only on group level) to 1 (classification on posture level, i.e. previously reported accuracy). Especially frequent but less relevant misclassifications between very similar postures within a group reduce the accuracy despite their potentially limited practical relevance. Consequently, we also take the group classification performance into account.

Fig. 8 shows the accuracy for posture detection and group detection for *RSS* and *MagCIR* as a function of the transmit power. The colored area between the respective lines shows the accuracy levels for intra-group error weights between 0 and 1. The *RSS* approach reaches up to $86\,\%$ group detection accuracy for $\bar{P}_{\mathrm{TX}} = 2.5\,\mu\mathrm{W}$. The *MagCIR* method achieves up to $90\,\%$ group detection accuracy and $80\,\%$ posture detection accuracy even for lower power levels.

VII. Conclusion

A realistic feasibility evaluation of WBAN-based posture detection for fall prevention requires a solid foundation of measurements for representative postures performed by various test subjects in realistic indoor environments. In this paper, we report an extensive and representative measurement campaign of the (18×18) channel impulse response matrix between 18 nodes mounted on different test subjects and measured in different environments. The 43 distinct postures have been selected with the application of fall prevention in mind. Based on these measurements we evaluate the posture detection performance of two previously proposed detectors [12]. These detectors have been chosen for low complexity and use either the total received signal energy (*RSS*, the energy of the impulse response for each link $\int |h(t)|^2 dt$) or the magnitude of the impulse responses (*MagCIR*, i.e. $|h(t)|$), thus simplifying signal processing and synchronization requirements. The sensitivity of *RSS* and *MagCIR* is analyzed w.r.t. frequency range and environment. We demonstrate that accuracies above $80\,\%$ can be achieved with low transmit power and noncoherent receivers within the UWB specifications using very few snapshot measurements as training data.

Acknowledgments

The authors would like to thank Bharat Bhatia and Upasana Chakraborty for their participation in the measurements.

References

[1] World Health Organization, "WHO Global Report on Falls Prevention in Older Age," 2008. [Online]. Available: https://apps.who.int/iris/handle/10665/43811

[2] Z. Zhang, C. Conly, and V. Athitsos, "A Survey on Vision-Based Fall Detection," in *Proceedings of the 8th ACM International Conference on PErvasive Technologies Related to Assistive Environments*, 2015.

[3] J. Pan and Y. Huang, "Intelligent fall prevention for Parkinson's disease patients based on detecting posture instabilily and freezing of gait," in *2015 12th International Conference on Informatics in Control, Automation and Robotics (ICINCO)*, vol. 01, 2015, pp. 608–613.

[4] L. Ren and Y. Peng, "Research of Fall Detection and Fall Prevention Technologies: A Systematic Review," *IEEE Access*, vol. 7, 2019.

[5] Z. Baird, S. Rajan, and M. Bolic, "Classification of Human Posture from Radar Returns Using Ultra-Wideband Radar," in *2018 40th Annual International Conference of the IEEE Engineering in Medicine and Biology Society (EMBC)*, 2018, pp. 3268–3271.

[6] Y. P. Zhang and Q. Li, "Performance of UWB Impulse Radio With Planar Monopoles Over On-Human-Body Propagation Channel for Wireless Body Area Networks," *IEEE Transactions on Antennas and Propagation*, vol. 55, no. 10, pp. 2907–2914, 2007.

[7] Q. Wang, T. Tayamachi, I. Kimura, and J. Wang, "An On-Body Channel Model for UWB Body Area Communications for Various Postures," *IEEE Transactions on Antennas and Propagation*, vol. 57, no. 4, pp. 991–998, 2009.

[8] X. Lu, X. Chen, G. Sun, D. Jin, N. Ge, and L. Zeng, "UWB-based Wireless Body Area Networks channel modeling and performance evaluation," in *2011 7th International Wireless Communications and Mobile Computing Conference*, 2011, pp. 1929–1934.

[9] M. Quwaider and S. Biswas, "Body Posture Identification Using Hidden Markov Model with a Wearable Sensor Network," in *Proceedings of the ICST 3rd International Conference on Body Area Networks*, no. 19, 2008.

[10] I. C. Paschalidis, W. Dai, D. Guo, Y. Lin, K. Li, and B. Li, "Posture Detection with Body Area Networks," in *Proceedings of the 6th International Conference on Body Area Networks*, 2011, pp. 27–33.

[11] X. Yang, M. Fang, A. Ren, Z. Zhang, Q. H. Abbasi, A. Alomainy, K. Mehran, and Y. Hao, "Reverse recognition of body postures using on-body radio channel characteristics," *IET Microwaves, Antennas & Propagation*, vol. 11, no. 9, pp. 1212–1217, 2017.

[12] R. Heyn and A. Wittneben, "Detection of Fall-Related Body Postures from WBAN Signals," in *GLOBECOM 2020 - 2020 IEEE Global Communications Conference*, 2020, pp. 1–6.

[13] S. Robinovitch, F. Feldman, Y. Yang, R. Schonnop, P. M. Leung, T. Sarraf, J. Sims-Gould, and M. Loughin, "Video capture of the circumstances of falls in elderly people residing in long-term care: an observational study," *The Lancet*, vol. 381, no. 9860, pp. 47 – 54, 2013.

[14] Rohde & Schwarz, *ZNBT Vector Network Analyzer Specifications*.